

## Diffusion of Mass in Liquid Metals and Alloys - Recent Experimental Developments and New Perspectives

Andreas MEYER and Florian KARGL

### Abstract

Despite its tremendous importance for the understanding of underlying mechanisms and for the input in modeling and simulation of processes alike, accurate experimental diffusion data in liquid metals and alloys are rare. Common techniques exhibit several drawbacks that in most cases prevent an accurate measurement of diffusion coefficients - convective contributions during diffusion annealing are the most prominent ones. Recently, we advanced the field of liquid diffusion experiments through the use of quasielastic neutron scattering (QNS) on levitated metallic droplets for accurate measurements of self-diffusion coefficients in high-temperature metallic liquids. For the accurate measurement of interdiffusion coefficients we combine long-capillary experiments with an in-situ monitoring of the entire interdiffusion process by the use of X-ray and neutron radiography. These experiments are accompanied by diffusion experiments in space in order to benefit from the purely diffusive transport under microgravity conditions. Recent experimental results are discussed in the context of the relation of self- and interdiffusion (Darken's equation) and of the relation of self-diffusion and viscosity (Stokes-Einstein relation).

**Keyword(s):** liquid metals, self-diffusion, interdiffusion, long-capillary, shear-cell, X-ray radiography, quasielastic neutron scattering.

### 1. Introduction

The study of diffusion processes in melts is vital for an understanding of liquid dynamics, nucleation, vitrification, and crystal growth. Diffusion coefficients are an essential input to the modeling of microstructure evolution and serve as a sound benchmark to molecular dynamics (MD) simulation results. In general, the self-diffusion coefficients of the individual components of a multicomponent liquid are related to the mean square displacement of the tagged atoms, whereas the interdiffusion coefficients are related to collective transport of mass driven by gradients in the chemical potential.

A common method to measure diffusion coefficients in liquid alloys is the long-capillary (LC) technique and its variations. There, a diffusion couple of different composition, in the case of interdiffusion, or containing a different amount of isotopes, in the case of self-diffusion, is annealed in the liquid state and subsequently quenched to ambient temperature. The diffusion profiles are analyzed post mortem. This technique exhibits several drawbacks that in most cases prevent an accurate measurement of diffusion coefficients.

Convective flow during diffusion annealing is recognized to be a severe problem in capillary experiments. Already small gradients in density, inherently present because of concentration gradients in interdiffusion experiments or caused by small gradients in temperature, result in additional contributions to the transport of mass between the diffusion couple due to flow. As

has been shown by comparison of LC diffusion experiments on ground with experiments under microgravity conditions <sup>1)</sup>, where buoyancy driven convective flow is suppressed, or with quasielastic neutron scattering (QNS) <sup>2)</sup>, where the presence of flow does not alter the measurement, resulting LC values on ground are systematically larger by several 10% to 100% compared to the real value (**Fig. 1**).

Relying on a post mortem analysis not only how convective flow alters the diffusion profile is unknown, but also the solidification of the sample itself poses a problem. In general, in alloys a more or less coarse grained microstructure is forming during crystallization that depends on the alloy composition, quench rates, and resulting temperature gradients. This alters the resulting concentration profiles on mm length scales and in many cases renders a post mortem analysis impossible. In addition, one has to retransform the coordinate of the determined concentration profile from the crystalline state at ambient temperature to the liquid state, which requires the knowledge of thermal expansions or absolute values of densities. If known at all, their experimental errors significantly reduce the precision of the diffusion coefficient. In long capillary diffusion experiments, the uncertainty in the knowledge of the absolute value of the annealing time poses an additional source of error. Therefore, accurate experimental diffusion data in liquid metals are rare and as a consequence a thorough understanding of atomic diffusion and its fundamental relations to other properties is still missing.

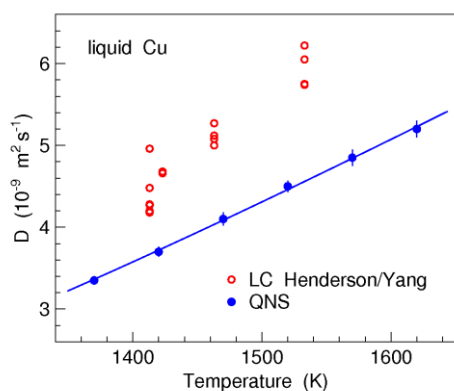


**Fig. 1** Self-diffusion coefficients in liquid copper from quasielastic neutron scattering (QNS) and from long-capillary (LC) tracer experiments <sup>3)</sup>. Figure reproduced from Ref. <sup>2)</sup>.

For the last six years we have invented / further developed an entire suite of new techniques for the investigation of diffusion in liquid metals and alloys at the DLR Institute of Materials Physics in Space. These techniques allow circumventing above mentioned restriction and as a consequence addressing the following open issues :

- Relation between self- and interdiffusion.
- Relation between self- and impurity diffusion.
- Elemental self-diffusion coefficients of an alloy.
- Dependence of diffusion on temperature.
- Dependence of diffusion on alloy composition.
- Relation of diffusion to viscous flow.
- Relation of diffusion to crystal growth.

In this review recent results of our work are highlighted and new perspectives for diffusion experiments under microgravity conditions are discussed.

## 2. New Experimental Techniques

### 2.1 Quasielastic Neutron Scattering

Recently, the field of liquid diffusion experiments advanced through the use of quasielastic neutron scattering (QNS) in combination with container-less processing for accurate measurements of self-diffusion coefficients in metallic liquids <sup>4)</sup>. QNS probes the dynamics of a liquid on atomic length scales and on a picosecond time scale, which is short enough to be undisturbed by the presence of convective flow (**Fig. 1**). It has been recently shown for the case of liquid Ge <sup>5)</sup>, that coherent contributions are separated in energy in the intermediate wavenumber ( $q$ ) range of QNS from incoherent contributions. Coherent contributions are either outside (Brillouin lines) the

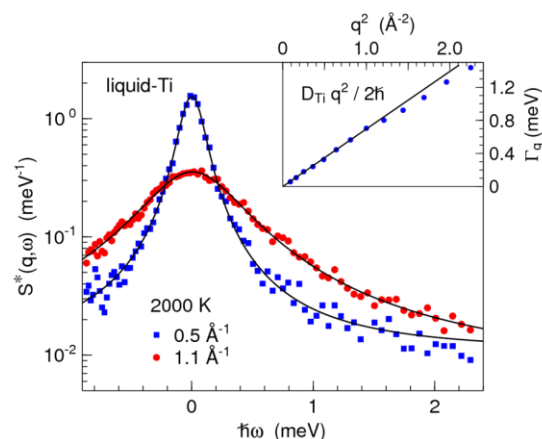


**Fig. 2** Quasielastic signal of liquid titanium as measured with neutron time-of-flight spectroscopy on an electromagnetically levitated sample (reproduced from Ref. <sup>9)</sup>). From the width of the quasielastic line,  $\Gamma_q$ , the self-diffusion coefficient can be obtained via  $D_{Ti} = 2\hbar\Gamma_q/q^2$  for small  $q$ .

dynamic range of QNS or appear as a flat background (central Rayleigh line) in the measured signal. In the case of a significant incoherent scattering contribution, e.g. from a liquid containing an adequate amount of Ni, Ti, or Cu, the QNS signal is also in most alloys dominated by the incoherent contributions. From the resulting incoherent intermediate scattering function the self-diffusion coefficient can be obtained on an absolute scale (**Fig. 2**). The combination of QNS with electromagnetic and electrostatic levitation of the sample enables the in-situ investigation of chemically reactive as well as of deeply undercooled metallic liquids <sup>6),7),8),9)</sup>.

Cu self-diffusion coefficients in liquid Cu are shown in **Fig. 1**. Our QNS results are compared to the LC data set by Henderson and Yang <sup>3)</sup> used as the text book reference for simulations in this system. In their LC experiment a relatively large scatter can be observed in the data and values are significantly above the QNS values. Their data set also exhibits an activation energy that is about 25% larger than for the QNS results. This indicates that the LC data are hampered by convective flow contributions during the diffusion annealing. Diffusion coefficients reported in classical and ab-initio MD simulations on liquid Cu exhibit a scatter of about +50% around our experimental values <sup>2)</sup>. This shows that, albeit MD simulation is a tool to reveal microscopic mechanisms, it is in general not applicable for the determination of absolute values of materials properties. On the other hand, accurate values of liquid diffusion coefficients from experiments can serve as a benchmark for the improvement of model potentials as has been recently shown for liquid Ti <sup>10)</sup>.

**Figure 3** displays self-diffusion coefficients in bulk-glass forming  $Pd_{40}Ni_{10}Cu_{30}P_{20}$  above its liquidus temperature. The temperature dependence of the Ni diffusion coefficient as measured with QNS exhibits a deviation from the usual Arrhenius-type (**Fig. 1**) and follows the prediction of mode

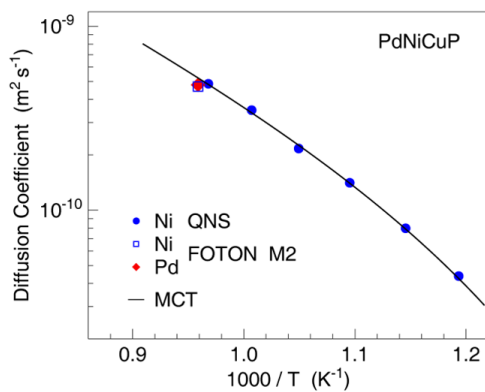


**Fig. 3** Self-diffusion coefficients in liquid Pd-Ni-Cu-P as measured with QNS (Ni) <sup>11)</sup> and in a shear-cell furnace aboard FOTON M2 (Ni and Pd) <sup>13)</sup>. Within experimental error bars the diffusion coefficients exhibit no size or mass dependence.

coupling theory <sup>11)</sup>. Self-diffusion coefficients in this alloy have also been measured under microgravity conditions in a shear-cell by applying isotopic substitution <sup>12)</sup>. Within error bars the Ni self-diffusion coefficient is equal to the QNS one. The comparably large and heavy Pd atoms exhibit a similar diffusion coefficient. Apparently, at least in this alloy, the transport mechanism is rather collective <sup>13)</sup>.

## 2.2 X-ray and Neutron Radiography

For the accurate measurement of interdiffusion we are currently establishing another technique: We combine LC experiments with an in-situ monitoring of the entire interdiffusion process by the use of X-ray and neutron radiography <sup>14),15)</sup>. After penetration of the X-ray or the neutron beam, respectively, through sample, holder and furnace, transmitted beam images are recorded by a flat panel detector.

The intensity profile along the long axis of the diffusion couple is transformed to a concentration profile via normalization to the intensity values of two reservoirs containing two standard reference compositions placed just above and below the sample. The detector is read out and reset in intervals of a few seconds thus resulting in a series of diffusion profiles. Hence, the interdiffusion process can be monitored as a function of time, from melting of the sample to its solidification. The concentration profiles obtained on the Al-Cu systems displayed in **Fig. 4** do not show obvious influences of convective flow. Apparently, the small capillary diameter in combination with the diffusion couples used here, that provide a sufficiently large difference in density, results in a stable density layering that in turn suppresses convective flow. A more detailed discussion on perspectives and especially on limitations of this new technique can be found in Ref. <sup>16)</sup>.

A first successful neutron experiment has just been performed at the ANTARES radiography beamline of the FRM-II <sup>15)</sup>. Using

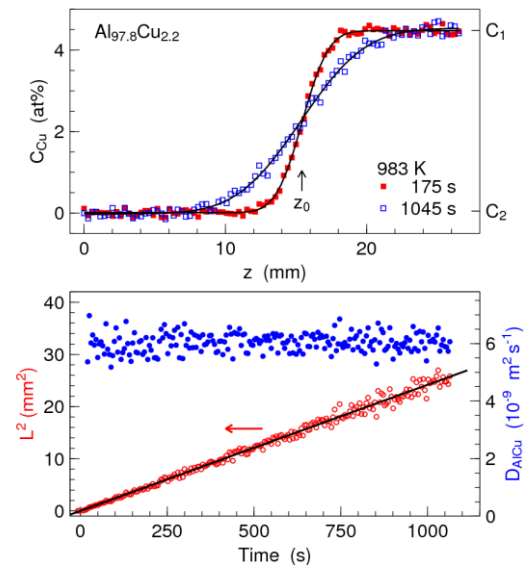


**Fig. 4** In-situ monitoring of interdiffusion in Al-Cu. Every 5 s an entire diffusion profile is measured (top). Analysis with the corresponding error function results in the diffusion length  $L$  as a function of time. The interdiffusion coefficient  $D_{AlCu}$  can be obtained from the slope of the square of  $L$  (bottom). Figure reproduced from Ref. <sup>14)</sup>.

neutrons, the radiographic contrast is in most cases complementary to that of X-rays and can even be changed by the use of proper isotopes. The in-situ monitoring paves the way for accurate measurements of transport coefficients, where one can rule out or eventually even correct for, convective contributions to the resulting concentration profiles, and where the experiment is not altered by the microstructure evolution during solidification. X-ray radiography of diffusion processes in liquid alloys is currently extended to the use on synchrotron radiation facilities, where the radiographic contrast of different components in an alloy depends on the selected wavelength of the monochromatic beam. This will allow the measurement of the different interdiffusion coefficients in a ternary alloy.

**Figure 5** shows self- and interdiffusion coefficients in  $Al_{80}Cu_{20}$ . The Cu self-diffusion in this alloy was measured with QNS - the interdiffusion with X-ray radiography. The interdiffusion coefficient is about a factor of 3 larger than the self-diffusion coefficient. A simple Ansatz to relate self- and interdiffusion goes back to Darken <sup>17)</sup>. The kinetic contributions to the interdiffusion coefficient  $D_{AB}$  are expressed by the self-diffusion coefficients  $D_A$  and  $D_B$  of the two components of the binary system, however, neglecting dynamic cross correlations <sup>18)</sup>:

$$D_{AB} = (C_B D_A + C_A D_B) \Phi \quad (1)$$

$C_A$  and  $C_B$  represent the alloy composition in at%. The thermodynamic factor  $\Phi$  is the 2<sup>nd</sup> derivative of the Gibbs free energy with respect to concentration and represents the

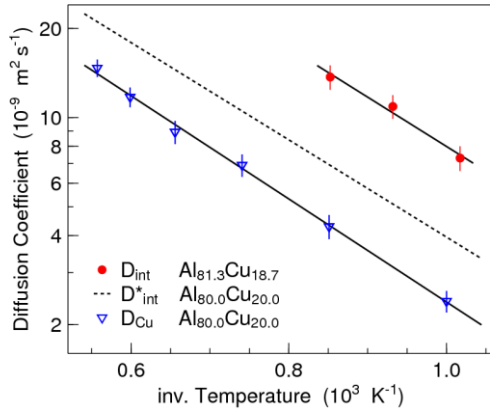


**Fig. 5** Self- and interdiffusion coefficients in  $\text{Al}_{80}\text{Cu}_{20}$ . The prediction of interdiffusion coefficients via Darken's equation (dashed line) fails to describe the experimental data under the assumption of  $D_{\text{Al}} \approx D_{\text{Cu}}$ . Figure reproduced from Ref. <sup>14</sup>.

contribution from a thermodynamic driving force. In  $\text{Al}_{80}\text{Cu}_{20}$  the resulting  $\Phi = 1.6$  is not large enough to account for the difference between self- and interdiffusion. Dynamic cross correlations further enhance interdiffusion with respect to the self-diffusion of the atoms by about a factor of 2. This shows that interdiffusion coefficients have to be measured and cannot be obtained from the knowledge of self-diffusion coefficients and the thermodynamic factor alone <sup>14</sup>.

Another common relation that is often taken for granted in order to calculate required self-diffusion coefficients of atoms or molecules in a liquid from the viscosity, or vice versa, is the Stokes-Einstein (SE) relation, <sup>19</sup>:

$$D \eta = (k_B T) / (6 \pi R_H) \quad , \quad (2)$$

where  $\eta$  is the viscosity,  $D$  the self-diffusion coefficient of the diffusing particles,  $R_H$  their hydrodynamic radius,  $T$  the absolute temperature, and  $k_B$  the Boltzmann constant.

The Stokes-Einstein relation was derived in order to study the diffusive motion of a mesoscopic sphere in a viscous medium <sup>20</sup>. However, in liquid metals and alloys the diffusing objects are of atomic size. Using the technique of electrostatic levitation, we measured Ni self-diffusion and viscosity of liquid  $\text{Zr}_{64}\text{Ni}_{36}$  in situ with high precision and accuracy <sup>21</sup>, over a broad temperature range spanning more than 800 K in which the values of mass transport are changing by 1.5 orders of magnitude. The inverse of the viscosity, measured via the oscillating drop technique, and the self-diffusion coefficient, obtained from quasielastic neutron scattering experiments, exhibit the same temperature dependence. It was found that  $D\eta = \text{const.}$  for the entire temperature range. This is contradicting the Stokes-Einstein relation, where  $D\eta \propto T$  (**Fig. 6**).

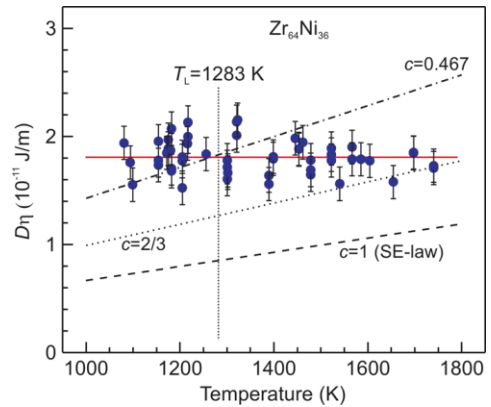


**Fig. 6** Ni self-diffusion coefficient times viscosity in  $\text{Zr}_{64}\text{Ni}_{36}$  versus temperature (symbols). The solid line is a guide to the eye. The dashed and dotted lines correspond to the Stokes-Einstein relation, Eq. (2), with different choices of the hydrodynamic radius ( $R_H \approx R_{\text{Ni}}$  for  $c = 1$ ). Figure reproduced from Ref. <sup>21</sup>.

### 3. Perspectives for Experiments in Space

The use of these in-situ techniques plays an essential role for advancements in the field of liquid diffusion: X-ray and neutron radiography for an in-situ monitoring of interdiffusion processes in long-capillary experiments, and quasielastic neutron scattering for accurate measurements of self-diffusion coefficients. However, both techniques are limited to selective systems, in which (only) one component exhibits a sufficient incoherent neutron scattering cross section, and in which stable density layering can be realized in long-capillary experiments, respectively.

Therefore, we initiated a series of *post-mortem* and *in-situ* diffusion experiments under microgravity conditions in order to reduce systematic errors due to gravity-induced flow- and sedimentation effects. Experiments under microgravity conditions should serve as a first benchmark for our earth-bound LC experiments and, in addition, should enable measurements of self- and interdiffusion coefficients on systems in which diffusion couples only exhibit an insufficient difference in density, and consequently, convective effects are expected to alter the measurement.

In this context we initiated the development of a compact X-ray apparatus (**Fig. 6**) <sup>22</sup>. This apparatus was designed as a second generation insert for the Materials Science Lab aboard the International Space Station (ISS) and currently adapted to our DLR sounding rocket MAPHEUS. This development includes a new high-temperature shear-cell (**Fig. 7**) <sup>23</sup>. It allows in-situ measurements via X-ray radiography due to the use of X-ray transparent materials as graphite and boron-nitride and its flat design. The shear-cell permits the samples to homogenize and equilibrate at the desired temperature before the diffusion process is initiated. Possible disturbing flow effects during



**Fig. 6** Compact and fully MSL compatible X-ray radiography insert for in-situ monitoring of interdiffusion processes under microgravity conditions – on the MAPHEUS sounding rocket and aboard the ISS.

melting are hereby avoided. A compact and sufficiently rugged design also enables experiments on a sounding rocket which inhibits buoyancy-driven fluid flow. A total of six samples with a diameter of 1.0 to 1.5 mm can be processed simultaneously.

For fast impurity and interdiffusion processes, where diffusion coefficients approach a value of  $10^{-8}\text{m}^2\text{s}^{-1}$ , a few minutes diffusion annealing suffice to obtain analyzable diffusion profiles. We built and space-qualified the ATLAS-M module (Atomic Transport in Liquid Alloys and Semiconductors)<sup>24</sup>. With ATLAS-M (**Fig. 8**) we succeeded to design a furnace set-up that combines fast heating, excellent isothermal conditions, and forced gas cooling at temperatures as high as 1100°C. On MAPHEUS ATLAS-M provides about 3 min annealing time in microgravity for measurements of impurity diffusion and interdiffusion in Ge and Al based alloys.

Building on the successful development of the shear-cell technique by Griesche and coworkers<sup>12</sup>, we are currently extending the accessible temperature range from 900°C to 1600°C (**Fig. 9**)<sup>25</sup>. Within the shear cell concept the long diffusion capillary is divided into segments, each adding a data

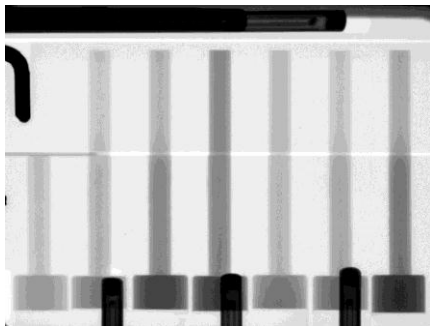


**Fig. 7** Ultra-small shear cell (40 mm x 40 mm x 19 mm) for interdiffusion experiments using X-ray radiography. Liquid Al-Ni capillary samples of different Ni concentration shortly after initiating the diffusion process by shearing the upper half to the right.



**Fig. 8** MAPHEUS short-time diffusion module ATLAS-M with 8 diffusion furnaces and the MAPHEUS experiment control unit (top). The module's outer radius is 356 mm.

point in a concentration profile. The two parts of the diffusion couple are molten and homogenized each in its part of the shear cell. This avoids sedimentation of small crystals during melting (as observed e.g. in Al-Ni with X-ray radiography). For the diffusion annealing the two parts of the diffusion couple are sheared together and subsequently the liquid diffusion profile is frozen in by segmenting the long capillary in the liquid. In such a way the diffusion profile is not altered by the microstructure formation upon crystallization and errors due to a length correction are not introduced. Applied under microgravity conditions, convection effects are suppressed and accurate self-, impurity, and interdiffusion coefficients can be obtained.

For the experimental investigation of diffusion of mass in liquid metals and semiconductors we already use *or we intend to use in the future* the following advanced and complementary techniques:

- QNS in combination with dedicated EML and ESL.
- X-ray and neutron radiography for the monitoring of interdiffusion processes.



**Fig. 9** Prototype of a 1600°C shear cell comprising of 30, 3 mm thick, shear segments (displayed up front) and bores for up to 6 long-capillary samples.

- Short-time experiments on impurity- and interdiffusion on MAPHEUS.
- X-ray radiography on sounding rockets *and in MSL aboard the ISS*.
- Shear-cell experiments in new high-temperature facilities on ground *and in space*.

#### 4. Conclusions

Quasielastic neutron scattering on levitated metallic droplets and long-capillary experiments in combination with X-ray or neutron radiography are new experimental tools that allow for an accurate and precise in-situ measurement of self- and interdiffusion coefficients. Experiments under microgravity conditions – shear-cell and in-situ with X-ray radiography – serve as a benchmark for earth-bound long-capillary experiments and, in addition, enable measurements on systems in which diffusion couples not exhibit a sufficient difference in density, and as a consequence, gravity driven convective contributions render the diffusion measurement impossible. First results show that commonly used text-book equations, i.e. Darken and Stokes-Einstein, are oversimplified and not valid in general. In the upcoming years research on diffusion of mass in liquid metals and alloys will further expand and new fundamental discoveries will be made that will also be crucial for the envisioned materials design from the melt. In this context, experiments in space will pose a central part of this development.

#### Acknowledgement

We thank our co-workers for a fruitful collaboration, the FRM-II for providing beam time for quasielastic neutron scattering and neutron radiography campaigns, and the German Ministry for Economy and Technology (BMWi) for funding through the Economic Stimulus Package I.

#### References

- 1) T. Masaki, T. Fukazawa, S. Matsumoto, T. Itami and S. Yoda: Meas. Sci. Technol, **16** (2005) 327, and references therein.
- 2) A. Meyer: Phys. Rev. B **104** (2010) 035902.
- 3) J. Henderson and L. Yang: AIME Trans, **221** (1961) 72.
- 4) A. Meyer, S. Stüber, D. Holland-Moritz, O. Heinen and T. Unruh: Phys. Rev. , B **77** (2008) 092201.
- 5) H. Weis, T. Unruh, A. Meyer: High Temp. High Phys. **42** (2013) 39.
- 6) A. I. Pommrich, A. Meyer, D. Holland-Moritz, T. Unruh: Appl. Phys. Lett., **92** (2008) 241922 and A. I. Pommrich, T. Unruh, A. Meyer: High Temp. High Press **42** (2013) 49.
- 7) S. Stüber, D. Holland-Moritz, T. Unruh, A. Meyer: Phys. Rev. B **81** (2010) 024204.
- 8) T. Kordel, D. Holland-Moritz, F. Yang, J. Peters, T. Unruh, T. Hansen, A. Meyer: Phys. Rev. B **83** (2011) 104205.
- 9) A. Meyer, J. Horbach, O. Heinen, D. Holland-Moritz, T. Unruh: Defect Diff. Forum **289-292** (2009) 609.
- 10) J. Horbach, R. Rozas, T. Unruh, A. Meyer: Phys. Rev., B **80** (2009) 212203.
- 11) A. Meyer: Phys. Rev. , B **66** (2002) 134205
- 12) A. Griesche, M.-P. Macht, S. Suzuki, K.-H. Kraatz, and G. Froberg: Scripta Mater, **57** (2007) 477.
- 13) A. Bartsch, K. Rätzke, A. Meyer, and F. Faupel: Phys. Rev. Lett. , **104** (2010) 195901.
- 14) B. Zhang, A. Griesche, A. Meyer: Phys. Rev. Lett., **104** (2010) 035902.
- 15) F. Kargl, M. Engelhardt, F. Yang, H. Weis, P. Schmakat, B. Schillinger, A. Griesche, A. Meyer: J. Phys. Condens Matter, **23** (2011) 254201.
- 16) F. Kargl, E. Sondermann, H. Weis, A. Meyer: High Temp. High Press **42** (2013) 3.
- 17) L. S. Darken: Trans. AIME **175** (1948) 184.
- 18) J. Horbach, S. K. Das, A. Griesche, G. Froberg, M.-P. Macht, A. Meyer: Phys. Rev. , B **75** (2007) 174304.
- 19) A. Einstein, Investigation on the theory of the Brownian movement, Dover, New York, 1926.
- 20) A. Einstein: Ann. Phys. **17** (1905) 549.
- 21) J. Brillo, I. Pommrich, A. Meyer: Phys. Rev. Lett., **107** (2011) 165902
- 22) F. Kargl, M. Balter, Ch. Stenzel, Th. Gruhl, N. Daneke, A. Meyer: J. Phys., Conf. Ser., **327** (2011) 012011.
- 23) C. Neumann, E. Sondermann, F. Kargl, A. Meyer: J. Phys. Conf. Ser., **327** (2011) 012052 and E. Sondermann, C. Neumann, F. Kargl, A. Meyer: High Temp. High Press **42** (2013) 23.
- 24) G. Blochberger, J. Drescher, C. Neumann, P. Penkert, A. Griesche, F. Kargl, A. Meyer: J. Phys. Conf. Ser. **327** (2011) 012051.
- 25) D. Heuskin, F. Kargl, A. Griesche, Ch. Stenzel, D. Mitschke, D. Bräuer, A. Meyer: J. Phys. Conf. Ser. **327** (2011) 012053.

(Received 29 Oct. 2012; Accepted 6 Jan. 2013)